NUMERICAL ALGEBRA,
CONTROL AND OPTIMIZATION

doi:10.3934/naco.2020029

# NEURO-FUZZY ACTIVE CONTROL OPTIMIZED BY TUG OF WAR OPTIMIZATION METHOD FOR SEISMICALLY EXCITED BENCHMARK HIGHWAY BRIDGE

Mostafa Ghelichi*, A. M. Goltabar and H. R. Tavakoli

Department of Civil Engineering
Noshirvani University of Technology, Babol, Iran

A. Karamodin

Department of Civil Engineering
Ferdowsi University of Technology, Mashhad, Iran

(Communicated by Gerhard-Wilhelm Weber)

Abstract. Control algorithms can affect the performance and cost-effectiveness of the control system of a structure. This study presents an active neuro-fuzzy optimized control algorithm based on a new optimization method taken from Tug of War competition, which is highly efficient for civil structures. The performance of the proposed control method has been evaluated on the finite element model of a nonlinear highway benchmark bridge; which is consisted of nonlinear structural elements and isolation bearings and equipped with hydraulic actuators. The nonlinear control rules are approximated with a five-layer optimized neural network which transmits instructions to the actuators installed between the deck and abutments. The stability of control laws are obtained based on Lyapunov theory. The performance of the proposed algorithm in controlling bridge structural responses is investigated in six different earthquakes. The results are presented in terms of a well-defined set of performance indices that are comparable to previous methods. The results show that despite the simple description of nonlinearities and non-detailed structural information, the proposed control method can effectively reduce the performance indices of the structure. The application of artificial neural networks is a privilege, which in so far as which, despite their simplicity, they have significant effects even on complex structures such as nonlinear highway bridges.

1. **Introduction.** Nowadays, in order to control the seismic behaviour of special structures such as bridges and buildings, the stability of which should not be at risk in earthquake, some techniques are widely utilized such as passive, semi-active and, active or hybrid control. The related studies are mainly grouped in two categories: (1) new control algorithms and (2) new control tools.

2010 *Mathematics Subject Classification.* Primary: 93C42; Secondary: 47N10.

*Key words and phrases.* Tug of war; Neural networks; ANFIS; Active control; Nonlinear base-isolated structures; Highway benchmark bridge.

The authors are supported by Babol Noshirvani university grant BNUT/370680/97.

* Corresponding author: Mostafa Ghelichi.

As far as the cost of using an active control system in the construction of a structure is extremely high, it is crucial to design an optimal algorithm as the brain of control system.

Benchmark models have been provided as a suitable platform for comparing the efficiency of the presented control methods. Benchmark problems were proposed in the structural response control, firstly in the mid-1990s [38]. Then, they dramatically developed in various fields such as seismically excited nonlinear buildings [34], wind-excited tall buildings [40], linear and nonlinear smart base-isolated structures [29–31, 37] and earthquake-excited cable-stayed bridge [3, 5].

A benchmark problem has been developed to control the seismically excited nonlinear highway bridge based on an actual bridge in Southern California [32, 39]. The reduction of bridge seismic responses with the installed friction piezoelectric dampers was investigated [26]. These dampers are more successful in controlling the bridge responses compared to MR dampers.

Instead of presenting control methods based on classical complex mathematical concepts to discover the nonlinear control rule, neural networks are presented which, despite their simplicity in computing, are very successful in this area. Since, in real-world applications, parameters of the mathematical formulation are due to uncertainty, different numerical approaches have been proposed based on neural networks to overcome the uncertainties. Basic Chance Constraint Programming (BCCP) and Robust Fuzzy Chance Constraint Programming (RFCCP) models are developed to handle uncertainties in both objective function and constraints. The superiority of RFCCP over BCCP model is proven through solving examples [25]. An adaptive active control algorithm was presented for controlling the benchmark nonlinear highway bridge [31]. Control force was calculated using a single layer nonlinearly neural network including a derivative type controller. The neural network was applied to estimate the nonlinear control laws rather than the system nonlinearities. The results showed that the presented method can reduce the structural responses. To study the effectiveness of MR dampers controlled by semi-active fuzzy controller subjected to near-fault ground motions, the genetic algorithm was used to optimize the fuzzy rules and the fuzzy controller membership functions [8]. The results indicated that the optimized fuzzy controller could effectively reduce the structural responses during near-fault earthquakes. Using neuro-fuzzy method as a control algorithm also has a great influence on the control of structural behavior [27].

Findings of these researches clearly indicate that the Neuro-fuzzy methods have a very acceptable performance as a controller especially in optimized mode.

Despite the fact that several meta-heuristic optimization methods have been presented, researchers have continued to improve the performance of these techniques [6, 7, 10, 15–19, 36].In an effort to obtain non-dominated Pareto optimal solutions, a novel meta-heuristic algorithm named Multi-Objective Dragonfly Algorithm was utilized to optimize grinding process considering a tri-objective mathematical model. The results revealed that the proposed algorithm is able to find non-dominated Pareto optimal solutions [21]. To solve the problem in medium and large search space size, two novel hybrid metaheuristic algorithms, Sine Cosine Crow Search Algorithm (SCCSA) and Water Cycle Moth Flame Optimization (WCMFO), are utilized. WCMFO uses very efficient operators which enable the algorithm to explore and exploit the solution space very efficiently and decrease the probability of trapping in local optima. [22]. Two novel meta-heuristics algorithms,

named grey wolf optimization (GWO) and moth-flame optimization (MFO), are utilized to solve the problems with different search space sizes. Based on the results, MFO functions better in small and medium instances in terms of percentage of relative error; meanwhile, GWO is better in terms of relative percentage of deviation in large-size test problems. [23]. A new hybrid algorithm called sinecosine crow search algorithm that inherits advantages of two recently developed algorithms, including crow search algorithm (CSA) and sinecosine algorithm (SCA) was presented. The exploration and exploitation capabilities of the proposed algorithm have significantly improved. [24].

Due to good performance of the adaptive neuro-fuzzy inference system (ANFIS) in pattern recognition problems, in the proposed method an ANFIS was used as a classifier at each level of separation which was trained by chaotic whale optimization algorithm (CWOA). Intelligent utilization of new extracted features, improving robustness of ANFIS and considering nine patterns in CCP recognition problem are the main contributions of the proposed method [14]. Furthermore, ANFIS was used to model the friction stir welding (FSW) process for automation. Few metaheuristic algorithms such as genetic algorithm (GA) and particle swarm optimization (PSO) were applied to ANFIS system to fine-tune the internal parameters of ANFIS and to make prediction more precise. PSO-ANFIS and GA-ANFIS models are in good agreement with the experimental results [13]. The very immediate-short-term to long-term influent flow rate are modelled and forecasted by a new developed hybrid model of ANFIS and Grey Wolf Optimizer (GWO). Concerning the influence of ANFIS parameters on the forecasting accuracy, these parameters are adjusted and optimized using Grey Wolf Optimizer (GWO). The results of this novel study demonstrate that reliable estimates of influent flow rate from 5-min up to 10 days in advance can be achieved using the developed direct and recursive hybrid GWO models [4]. Artificial intelligence tools are improved with various meta-heuristic algorithms including Particle Swarm Optimization (PSO), Genetic Algorithm (GA), Invasive Weed Optimization (IWO), and Cultural Algorithm (CA) for accurate prediction of demand for dairy products. From these, PSO exhibits a better performance in feature selection and IWO shows the best performance in improving the prediction tools by achieving the lowest error [9].

In a recent research, a new meta-heuristic population-based optimization algorithm was introduced based on tug of war competition [20]. In this method, each solution candidate is considered as a team that should participate in a series of competitions. The numerical results have indicated that the Tug of War Optimization (TWO) method has a better performance compared to other common methods. In the present paper, given the expressed benefits of a neuro-fuzzy controller and the appropriate performance of tug of war optimization approach, a new active optimized controller is presented. Because of sever nonlinearity in bridge model and uncertainties in predicting control laws, according to the results concluded from literature, the stability of the control system is expected to increase with the proposed method. Moreover, according to the results, the controller's performance has improved during various earthquakes and seismic responses have considerably decreased compared to conventional methods.

This paper is organized as follow: the second section presents the dynamical formulation of highway benchmark bridge structure. The details of the optimization method are presented in the third section. The results of the simulation studies of

the proposed method on the benchmark structure and discussion of key results are presented in the fourth section, followed by the conclusions.

2. **Benchmark highway bridge.** A schematic of the benchmark structure considered in this study is shown in Fig. 1 [1]. The bridge structure is modeled after the newly constructed 91/5 (m) over-crossing in Orange County, Southern California. This bridge is pre-stressed concrete, box-girder type. For a detailed description of the structure, the readers can refer to the definition paper [1, 39]. Owing to its location, this bridge is likely exposed to severe near-fault ground motions. No seismic isolators have been used in its original construction. In order to improve the seismic performance, for the purposes of the phase I benchmark study, the bridge is isolated using four seismic isolators at each of the east and west abutments. Additionally, for phase II of the benchmark study, the bridge deck is also isolated at the two columns (north and south) using one isolator for each. In the present study, phase I of the structure has been investigated. The soilstructure interaction effects are included at both the abutments using linear springs and viscous dashpots. The vertical columns also exhibit nonlinear behavior, making this structure highly nonlinear. The finite-element model of the bridge (evaluation model) has 430 degrees of freedom. The nonlinearity in the structure is attributed to the behavior of the center columns and the isolation elements. The moment-curvature relationship of the two columns has been modeled by a bilinear hysteresis model. Other force-displacement relationships, such as axial, shear, and torsion are assumed to be linear. Moreover, in order to model the material nonlinearity in the columns, a concentrated plasticity model has been used.

The equations of motion (assumed for controller development only) for this system, in both the orthogonal directions, can be written as:

$$\begin{aligned} M\Delta\ddot{U}(t) + C\Delta U(t) + K(t)\Delta U(t) \\ = M\eta\Delta\ddot{U}_g(t) + b\Delta F(t), \end{aligned} \tag{1}$$

where $\Delta U$ is the incremental displacement vector; $\ddot{U}_g$ is the vector of ground accelerations, including two horizontal components; and $\Delta F(t)$ is the incremental control force. $\eta$ and $b$ are loading vectors for the ground acceleration and control forces, respectively and $M$ is the mass matrix. The stiffness matrix of the structure, $K(t)$ , consists of the linear part $K_L$ and nonlinear part $K_N(t)$ . Eq. (1) can be solved using the general Newmark integration method. The active devices used in this study are modelled as ideal hydraulic actuators. The ideal actuator is assumed to be able to instantly and accurately supply the force commanded by the control algorithm. The control oriented model is given as:

$$\begin{aligned} \dot{X}^r &= A_r X_r + B_r u + E_r \ddot{u}_g \\ y_z &= C_r^z X^r + D_r^z u + F_r^z \ddot{u}_g \\ y_m &= C_r^m X^r + D_r^m u + F_r^m \ddot{u}_g + v, \end{aligned} \tag{2}$$

where the subscript $r$ in Eq. (2) refers to the reduced model. In the above equations, $X$ refers to the states of the system, $A$, $B$ and $E$ are the system state matrices, $\ddot{u}_g$ is the ground acceleration vector in two directions. $y_z$ is the regulated output and $y_m$ is the measurement output. The matrices $C$, $D$ and $F$ are mapping matrices of appropriate dimensions and $v$ denotes the measurement noise. The finite element model of the bridge is shown in Fig. 2.

## 3. Tug of war optimization.

### 3.1. Idealized framework of tug of war.

Tug of war is a strength contest in the rope pulling. Two competing teams are in an attempt to pull a rope to bring it to their own side. Naturally, the amount of the losing team displacement determines the amount of rope displacement. A tug of war tournament is shown in Fig. 3.

An idealized framework is utilized in this paper where the teams with the weights of $w_i$ and $w_j$ are considered as two objects lying on a smooth surface as shown in Fig. 4.

$\mu_k$ is the coefficient of kinematic friction and $\mu_s$ is the coefficient of static friction. As a result of rope pulling, two opposite and equal forces ($F_P$) are applied to the teams according to the third law of Newton. Until the pulling force for an object $i$ is smaller than the maximum force of static friction ($W_i\mu_s$),it rests in its initial place. Otherwise, the resultant force is non-zero and can be calculated as:

$$F_r = F_p - W_i\mu_k. \tag{3}$$

As a result, according to the second law of Newton, the object $i$ moves towards the object $j$ with the acceleration of:

$$a = \frac{F_r}{W_i/g}. \tag{4}$$

Since the start velocity of movement of an object $i$ is zero, its new location can be calculated as:

$$X_i^{new} = \frac{1}{2}at^2 + X_i^{old}. \tag{5}$$

### 3.2. The algorithm of optimization.

Each candidate's answer $X_i = x_{i,j}$ in T-WO population-based algorithm is considered as a team in a series of competitions. The teams weight is defined based on the corresponding solution quality, and the pulling force value of a team in the competition is considered to be proportional to its weight. The lighter team moves to the heavier team so the convergence operator of this method is formed. The step-by-step algorithm of TWO can be expressed as follows:

**• Step1: Initialization**

A population of $N$ initial solutions that contain the location of actuators is generated randomly:

$$x_{i,j}^0 = x_{j,min} + rand(x_{j,max} - x_{j,min}) \ , \ j = 1, 2, ..., N, \tag{6}$$

where $x_{i,j}^0$ is the $jth$ variable initial value for the $ith$ candidate answer; $x_{j,min}$ and $x_{j,max}$ are the permissible values of the lower and upper bounds for the $jth$ variable, respectively; $rand$ is a random number from a uniform distribution in the interval [0,1]; and $N$ is the number of optimization variables.

**• Step 2: Evaluation of candidate plans and weight assignment**

The values of the objective function (introduced in Sect. 4) for the candidate answers are evaluated by ATF (Active Tug of war Fuzzy proposed method) control algorithm. The initial answers are sorted and saved in a memory named as league. The weight of each answer is considered as follow:

$$W_i = \frac{fit(i)_j - fit_{worst,j}}{fit_{best,j} - fit_{worst,j}} + 1 \ , \ i = 1, 2, ..., N \ , \ j = 1, 2, ..., O, \tag{7}$$

where $fit(i)$ is the value of fitness for the $ith$ particle; $fit_{worst}$ and $fit_{best}$ are the values of fitness for the worst and best candidate answers of the current iteration. $O$ is the number of objectives. According to Eq. (7) the teams weights range between 1 and 2.

**•Step 3: Competition and displacement**

Each of the league teams compete with each other one by one in each iteration to move to its new position. The pulling force applied by a team is equal to its static friction force ($W\mu_s$). Therefore, the pulling force existing between two teams $i$ and $j$ ($F_{p,ij}$) can be calculated as $max\{W_i\mu_s, W_j\mu_s\}$. Such a definition keeps the position of the heavier team unaltered. When team $i$ interacts with heavier team $j$ in the $kth$ iteration, the resultant force can be calculated as follows:

$$F^k_{r,O,ij} = F^k_{p,ij} - W^k_i\mu_k. \tag{8}$$

As a result, team $i$ moves towards the team $j$ with the acceleration of:

$$a^k_{ij} = (\frac{F^k_{r,ij}}{W^k_i\mu_k})g^k_{ij}, \tag{9}$$

where $a^k_{ij}$ is the value of the team $i$ acceleration towards the team $j$ in the $kth$ iteration; $g^k_{ij}$ is the constant of gravitational acceleration defined as:

$$g^k_{ij} = X^k_j - X^k_i, \tag{10}$$

where $X^k_i$ and $X^k_j$ are the vectors of position for candidate answers $i$ and $j$ in the $kth$ iteration. Finally, after the competition of two teams $i$ and $j$, the displacement of the team $i$ can be calculated as:

$$\Delta X^k_{ij} = \frac{1}{2}a^k_{ij}\Delta t^2 + \alpha^k\beta(X_{max} - X_{min})randn(1,n). \tag{11}$$

The second term in Eq. (11) is considered as a random part of the algorithm. The role of $\alpha^k$ is to gradually decrease the random part of the team's movement. $\alpha$ for common applications could be chosen as a constant from the interval [0.9, 0.99]; the algorithm convergence speed decreases as the $\alpha$ value increases and help the candidate answers investigate the search space more rigorously. $\beta$ can be chosen as a scaling factor from the interval (0, 1]. The steps of the candidate answers during moving in the search interval are controlled by this parameter. When there is a need to search with smaller steps, it is supposed to choose smaller values for this parameter. $X_{max}$ and $X_{min}$ are the bounds of the permissible ranges of the design variables. Therefore, the total displacement of the team $i$ in iteration $k$ is equal to ($i \neq j$):

$$\Delta X^k_i = \Sigma^O_{t=1}\Sigma^N_{j=1}\Delta X^k_{ij}. \tag{12}$$

So at the end of the $kth$ iteration, the new position of team $i$ is then calculated as:

$$X^{k+1}_i = X^k_i + \Delta X^k_i. \tag{13}$$

**•Step 4: League updating**

Once a full competition cycle was made between all the teams, the league should be updated by comparing the current league teams with the new candidate answers. Each of new candidate answers or Nth league team that is weaker in terms of the value of the objective function shall be removed from the competition.

**•Step 5: Handling the side constraints**

It is important to have a compensatory solution when a candidate answer leaves the search space. This situation often occurs when $\delta X$ for a lighter team is usually bigger. The global best answer method is used in this paper. In the $kth$ iteration, the following formulation is used to define the new value for the $jth$ optimization variable from the $ith$ team that crossed the side constraints:

$$X_{ij}^{k} = GB_j + \frac{randn}{k}(GB_j - x_{ij}^{(k-1)}), \tag{14}$$

where $GB_j$ is the $jth$ variable from the global best answer that has ever been obtained.

**•Step 6: Termination**

Steps 2 to 5 must be repeated until an ending criterion is met. . For more detailed information about the application of tug of war optimization method refer to [20].

4. **Selection of objective functions.** To design and optimize the proposed active control algorithm a single-objective optimization process is performed. As far as the objective of the control system is to improve the seismic responses of the bridge with the priority of the base shear and considering the impact of the bridge acceleration on its base shear, the output of the fitness function must be the maximum base shear of the bridge or its maximum acceleration. To this end, the output of the fitness function for each of the accelerograms considered for optimization is one criterion related to maximum base shear (J1) and again the criterion for maximum acceleration (J4).

1. Option 1: The maximum of peak base shear force in the controlled structure among all six earthquakes imposed to the bridge, normalized by the corresponding shear in the uncontrolled structure;

$$J1 = \underbrace{Max}_{\substack{\text{Elcentro}\\ \text{Northridge}\\ \text{ChiChi}\\ \text{NPlamSp}\\ \text{TorkBolu}\\ \text{Kobe-NIS}}} \left\{ \frac{max_{i,t}|F_{bi}(t)|}{F_{0b}^{max}} \right\}, \tag{15}$$

   where $F_{bi}(t)$ is the base shear in the controlled structure and $F_{0b}^{max}$ is the maximum peak base shear force in the uncontrolled structure.
2. Option 2: The maximum of peak acceleration at mid-span of the controlled structure among all six earthquakes imposed to the bridge, normalized by the corresponding mid-span acceleration of the uncontrolled structure;

$$J4 = \underbrace{Max}_{\substack{\text{Elcentro}\\ \text{Northridge}\\ \text{ChiChi}\\ \text{NPlamSp}\\ \text{TorkBolu}\\ \text{Kobe-NIS}}} \left\{ max_{i,t}|\frac{\ddot{y}_{mi}(t)}{\ddot{y}_{0m}^{max}}| \right\}, \tag{16}$$

   where $\ddot{y}_{mi}(t)$ is the mid-span acceleration of the controlled structure and $\ddot{y}_{0m}^{max}$ is the maximum mid-span acceleration of the uncontrolled structure.

It is necessary to control that optimization based on minimization of which of above mentioned criteria will result in better seismic control of the bridge. This will be discussed after the results in Section 6.

## 5. Proposed control scheme.

The active tug of war-fuzzy optimized (ATF) controller consists of two internal optimized ANFIS controllers; one for controlling the seismic behavior of the bridge exposed to far-field earthquakes known as F-ANFIS and the other for controlling the seismic behavior of the bridge exposed to near-field earthquakes known as N-ANFIS.

### 5.1. Earthquake observer.

One of the issues affecting the seismic behavior of the structures is the nature of far-field or near-field earthquake. The distinctions between near-field and far-field earthquakes are features such as high-velocity pulses and long-period displacement [28]. In this study, the ground velocity is selected as the distinction between far-field and near-field earthquakes. By defining two S-shaped (near-field function named NF) and Z-shaped (far-field function named FF) fuzzy membership functions, whose inputs consist of maximum velocity of ground motions in last 3 seconds, the contribution of each internal controller in the calculation of the amount of the control force is determined. The force of each actuator is obtained from the following equation:

$$F = \frac{w_N F_N + w_F F_F}{w_N + w_F}, \tag{17}$$

where $F$ is the final force calculated by the earthquake observer, $F_N$ is the force obtained from the optimized controller for the near-field earthquakes, $F_F$ is the force obtained from the optimized controller for the far-field earthquakes, $w_N$ and $w_F$ specify the weight of the magnitude of near-field and far-field earthquakes which is the membership degree of the input velocity to the observer in the $NF$ and $FF$ fuzzy functions. Regarding [12], maximum velocity of the ground motions in near-field earthquakes usually reaches 0.5 m/s. Accordingly, the fuzzy functions $FF$ and $NF$ are defined in a way that:

1. At the velocity of 0.5 m/s, the membership degree in both functions becomes 0.5. In other words, for the mentioned velocity, the ratio of each of the two internal controllers in force determination would be 50%.
2. For the velocities less than 0.425, the earthquake is considered fully far-field.
3. For the velocities more than 0.575, the earthquake is considered fully near-field.

The contribution of each internal controller in calculation of the force is determined separately for each of the directions based on Eq. (17). The membership functions of earthquake observer are shown in Fig. 5.

### 5.2. Inputs.

In order to avoid complexity and considering the accuracy required to achieve the optimal solution, two inputs are considered for the desired controller as follows:

1. The normalized acceleration, which is calculated based on the accelerometers measured values. As far as the values are between -10 and +10 in volts after passing through A/D converter, the normalized acceleration as the first ANFIS controller input is obtained in range $[-1 \ +1]$ by multiplying these values by 0.1.

2. The normalized displacement, which is calculated based on the measured values of the displacement gauges. As far as the values are between -10 and +10 in volts after passing through A/D converter, the normalized displacement as the second ANFIS controller input is obtained in range $[-1\ +1]$ by multiplying these values by 0.1.

5.3. **Input membership functions.** Six Gaussian membership functions are considered for each of the internal ANFIS controller inputs. The values of the membership functions parameters are shown in Table 1 and Fig. 6.

TABLE 1. Input membership functions parameters in ANFIS controller

| | N1 | N2 | N3 | P1 | P2 | P3 |
|---|---|---|---|---|---|---|
| $\sigma$ | 0.15 | 0.15 | 0.15 | 0.15 | 0.15 | 0.15 |
| C | -1.0 | -0.6 | -0.2 | 0.2 | 0.6 | 1.0 |

5.4. **Result functions.** The output of the controller is the normalized force in range [0 1], multiplication of which by maximum applied forces of actuators (100 KN), gives the required force for each actuator. Each ANFIS network used in the controller consists of 36 result functions. The values of the parameters of these functions for each internal controller are obtained following optimization by TWO algorithm.

5.5. **Optimization of internal ANFIS controllers.** To optimize the responses of the internal F-ANFIS controller as the far-field earthquake, four accelerograms have been selected including El-Centro earthquake with the coefficients of 1 and 1.5 and North Palm Springs earthquake with the coefficients of 1 and 1.5. Then, the optimization process and adjustment of the parameters are separately performed for each of these accelerograms. Finally, the optimized controller with the best performance in far-field earthquakes is selected. Similarly two accelerograms are chosen for the near-field earthquake including Northridge earthquake with the coefficients of 1 and 1.5.

The result functions in ANFIS are zero or first-order functions. In this paper linear result functions are used in ANFIS controller as Eq. (18):

$$f_i = p_i x + q_i y + r_i \ \ i = 1, 2, ..., 36, \tag{18}$$

where $x$ is the first network input (normalized acceleration), and $y$ is the second input (normalized displacement). $p$, $q$, and $r$ are parameters of $ith$ result function. These parameters are teams in the presented optimization algorithm. So, the number of input parameters to the optimization algorithm for the controller adjustment is 108. optimization of each internal ANFIS controllers is performed through optimization algorithm and adjusting the parameters of the resulted functions (Eq. (18) in N-ANFIS or F-ANFIS controllers). The optimization results will be discussed in Sect. 6. In this process, the numerical model of the bridge with the proposed control system should be taken under a desired earthquake and coded as a fitness function. Fig. 7 shows ANFIS configuration of the proposed controller. The applied methodology to design an active neuro-fuzzy optimized controller is presented in Fig. 8.

5.6. **The stopping criteria of optimization.** One of the major problems in optimization method is the choice of an adequate stopping rule. In this article, the following three terms have been selected as the stopping criteria:

1. The maximum number of generations is equal to 50.
2. The minimum objective function is equal to zero.
3. Generational recession is equals to fifteen generations.

6. **controllers optimization results.** Tables 2 and 3, respectively show the results of the optimization process for F-ANFIS and N-ANFIS controllers based on criteria J1 and J4, separately (as described in Sect. 4). In order to make it possible to decide on the superiority of the optimization criteria the values for three of the bridge response indices (J1, J3, J5) are considered. The comparison of eight different cases listed in Table 2 implies, that the optimized controller under Palm Springs earthquake with the coefficient of 1.5 and based on the minimization of J1 criterion, with higher success rate compared to other scenarios, could optimally reduce other criteria as a far-field controller. Fig. 9 shows the optimization process in the mentioned scenario.

Furthermore, by the comparision of four different cases listed in Table 3, shows that the optimized controller has been more successful in reducing the response indices as a near-field controller under Northridge earthquake with the coefficient of 1.5 and based on the minimization of J1 criterion. Fig. 10 shows the optimization process in the mentioned scenario.

TABLE 2. The mean of criteria J1, J3 and J5 in a far-field earthquake, for different optimization scenarios of ANFIS controller (F-ANFIS).

| Optimization by minimizing criterion J1 | | | | |
|---|---|---|---|---|
| Earthquake | EL-Ce×1 | EL-Ce×1.5 | N.P.Spr.×1 | N.P.Spr.×1.5 |
| J1 | 1.1198 | 1.1153 | 0.8942 | 0.8867 |
| J3 | 0.6153 | 0.5235 | 0.8856 | 0.8171 |
| J5 | 0.3586 | 0.2684 | 0.6125 | 0.5928 |
| Optimization by minimizing criterion J4 | | | | |
| Earthquake | EL-Ce×1 | EL-Ce×1.5 | N.P.Spr.×1 | N.P.Spr.×1.5 |
| J1 | 1.1336 | 1.1295 | 0.8895 | 0.9459 |
| J3 | 0.5983 | 0.5467 | 0.8763 | 0.8543 |
| J5 | 0.3347 | 0.2733 | 0.5826 | 0.6372 |

The results of structural analysis of the bridge under 6 earthquakes with the proposed controller have been presented in Table (4). Moreover, in order to make a comparison and verify the results, J1 and J4 performance indices are plotted in Figs. 11, 12, and 13 along with the results of previous studies. The methods compared in these figures are as follows:
ATF: Active Tug of War Fuzzy Proposed Method.
P-SAMP: Passive Sample Control Method [39].
A-SAMP: Active Sample Control Method [39].
A-ANF: Active ANFIS Controller [2].
SA-AFSMC: Semi Active Adaptive Fuzzy Sliding Mode Control [33].
SA-CLOP: Semi Active Sample Control Method [39].

TABLE 3. The mean of criteria J1, J3 and J5 in a Near-field earthquake, for different optimization scenarios of ANFIS controller (N-ANFIS).

| Optimization by minimizing criterion J1 | | |
|---|---|---|
| Earthquake | Northridge×1 | Northridge×1.5 |
| J1 | 0.7321 | 0.7125 |
| J3 | 0.3988 | 0.3846 |
| J5 | 0.3833 | 0.3644 |
| Optimization by minimizing criterion J4 | | |
| Earthquake | Northridge×1 | Northridge×1.5 |
| J1 | 0.7466 | 0.7389 |
| J3 | 0.4038 | 0.6089 |
| J5 | 0.3957 | 0.4782 |

TABLE 4. The results of the proposed controller.

| | NPalmspr | ChiChi | El Centro | Northridge | TurkBolu | Kobe-NIS | Avg |
|---|---|---|---|---|---|---|---|
| J1:Pk. base Shear | 0.925 | 0.652 | 0.678 | 0.729 | 0.697 | 0.892 | 0.762 |
| J2:Pk. Over.Mom. | 0.693 | 0.878 | 0.595 | 0.786 | 0.587 | 0.547 | 0.681 |
| J3:Pk. Mid. Disp. | 0.684 | 0.701 | 0.667 | 0.572 | 0.661 | 0.607 | 0.648 |
| J4: Pk. Mid. Acc. | 0.997 | 0.912 | 0.788 | 0.783 | 0.812 | 0.822 | 0.852 |
| J5: Pk. Bear. Def. | 0.546 | 0.554 | 0.563 | 0.514 | 0.605 | 0.451 | 0.538 |
| J6: Pk. Ductility | 0.647 | 0.517 | 0.576 | 0.547 | 0.186 | 0.585 | 0.509 |
| J7: Dis. Energy | 0.000 | 0.087 | 0.000 | 0.120 | 0.05 | 0.000 | 0.042 |
| J8: Plas. Connect. | 0.000 | 0.500 | 0.000 | 0.500 | 0.000 | 0.000 | 0.166 |
| J9:Nor.Base shear | 0.839 | 0.567 | 0.610 | 0.594 | 0.743 | 0.718 | 0.678 |
| J10:Nor.Over. Mom. | 0.561 | 0.597 | 0.642 | 0.686 | 0.459 | 0.745 | 0.615 |
| J11: Nor. Mid. Disp. | 0.611 | 0.487 | 0.504 | 0.473 | 0.514 | 0.639 | 0.538 |
| J12: Nor. Mid. Acc. | 0.798 | 0.694 | 0.568 | 0.681 | 0.842 | 0.765 | 0.724 |
| J13: Nor. Bear. Def. | 0.397 | 0.456 | 0.415 | 0.616 | 0.214 | 0.324 | 0.404 |
| J14: Nor. Ductility | 0.615 | 0.623 | 0.561 | 0.802 | 0.123 | 0.683 | 0.567 |
| J15: Pk. Con. Force | 0.010 | 0.024 | 0.007 | 0.025 | 0.018 | 0.012 | 0.016 |
| J16: Pk. Stroke | 0.509 | 0.517 | 0.518 | 0.452 | 0.580 | 0.451 | 0.504 |
| J17: Pk. Power | 0.037 | 0.110 | 0.024 | 0.098 | 0.077 | 0.029 | 0.063 |
| J18: Total Power | 0.010 | 0.014 | 0.005 | 0.017 | 0.015 | 0.015 | 0.012 |
| J19:No.Con. Devices | 16 | 16 | 16 | 16 | 16 | 16 | 16 |
| J20: No. Sensors | 12 | 12 | 12 | 12 | 12 | 12 | 12 |
| J21:Comp. Resources | 16 | 16 | 16 | 16 | 16 | 16 | 16 |

As shown in Table 4, the proposed optimized control method has effectively reduced the bridge performance indices using the same control devices as of pervious researches [1]. The following points can be concluded;

- The proposed algorithm reduced the bridge peak base shear, overturning moment, mid-span displacement, mid-span acceleration, normed base shear and normed mid-span acceleration under various earthquakes up to 35%. Among these, the mid-span acceleration index (J4) had the lowest reduction (15%).
- The peak bearing deformation, ductility, normed overturning moment, normed mid-span displacement, normed bearing deformation, and normed ductility indices decreased by 40 to 60%, during the optimized control process. Among these, the normed bearing deformation index (J13) showed the largest decrease (60%).
- One of the prominently visible features of the proposed method is decrease in the structural damage. Since the parameters such as curvature created in columns, energy absorbed by nonlinear behavior and hysteresis loops and the number of plastic joints directly affect the structural damage, the criteria containing these parameters will be appropriate to measure the structural

TABLE 5. Results of the Friedmans test.

| Responce indices | Friedmans mean rank | | | | | | *P* value |
|---|---|---|---|---|---|---|---|
| | ATF | P-SAMP | A-SAMP | A-ANF | SA-CLOP | SA-AFSMC | |
| J1 | 1.6 | 5.2 | 5.6 | 1.8 | 4 | 2.8 | 8.95E-04 |
| J2 | 1.2 | 1.8 | 4.6 | 5.4 | 4.4 | 3.6 | 1.10E-03 |
| J3 | 1.4 | 1.6 | 5 | 4.7 | 4.7 | 3.6 | 2.00E-03 |
| J4 | 3.8 | 5.9 | 1.4 | 1.7 | 3.2 | 5 | 3.34E-04 |
| J5 | 2 | 1.8 | 5.5 | 5.5 | 4 | 2.2 | 2.16E-04 |
| J6 | 1.2 | 1.8 | 5.5 | 3.9 | 5.3 | 3.3 | 4.07E-04 |
| J7 | 1.4 | 1.6 | 4.9 | 5.6 | 4.5 | 3 | 3.80E-04 |
| J8 | 1.2 | 1.8 | 4.1 | 4.8 | 3.5 | 5.6 | 4.95E-04 |
| J9 | 2.9 | 1.9 | 4.3 | 4.6 | 4.1 | 3.2 | 1.67E-01 |
| J10 | 2 | 2 | 5 | 6 | 4 | 2 | 3.78E-04 |
| J11 | 1.4 | 1.6 | 5.5 | 3.9 | 5 | 3.6 | 7.31E-04 |
| J12 | 1.4 | 5.7 | 2.1 | 2.5 | 4 | 5.3 | 3.87E-04 |
| J13 | 2.6 | 1 | 5 | 6 | 4 | 2.4 | 1.89E-04 |
| J14 | 3.3 | 2.9 | 6 | 2.8 | 5 | 1 | 4.02E-04 |
| J15 | 5.3 | 5 | 1.5 | 2 | 2.7 | 4.5 | 4.02E-04 |
| J16 | 2.2 | 1 | 5 | 6 | 4 | 2.8 | 4.02E-04 |
| Average | 2.18 | 2.66 | 4.43 | 4.20 | 4.15 | 3.38 | |
| SD | 1.15 | 1.72 | 1.46 | 1.58 | 0.67 | 1.25 | |

damage. Thus, J6, J7, J8 indices can indicate the potential for structural damage to the bridge.

7. **Statistical analyses.** To make a reliable conclusion and to show the superiority of the proposed control algorithm over state-of-the-art algorithms, in this section, statistical tests are carried out. A multiple comparison test (Friedmans test) is performed to determine significant differences between the properties of the control algorithms. The average rankings obtained by Friedman test are used to show that how successful is the proposed control ATF algorithm. Based on the Friedmans test rankings, the lower the rank, the more efficient the algorithm is. Table 5 presents the mean ranks obtained by this test at 95% confidence level. Based on the average and standard deviations, the ATF algorithm is the best solution method which outperforms other state-of-the-art algorithms in majority of the test problems. Fig. 14 presents a view of the results of the Friedmans test. Based on Fig. 14, it becomes obvious that the ATF not only is the best solution method among other state-of-the-art algorithms, but also is the most robust solution methodology comparing to the other solution methods. For this purpose, comparing the worst ranking of the ATF to other algorithms, it has the lowest worst rank among the algorithms. Therefore, it can be inferred that the ATF is the most robust solution methodology which performs well in all types of structural response indices.

8. **Conclusions.** The performance of a new optimized Nero-fuzzy controller for the active control of the benchmark highway bridge with bi-linear isolation system has been investigated. The advantages of the proposed control process are as follow: it does not require complicated control rules, it does not need accurately defining mathematical model of structure, and it has good ability to deal with the uncertainties including input loading or structural parameters. Adaptive control laws are derived using an ANFIS controller, whose output parameters are adjusted by the meta-heuristic tug of war optimization algorithm. ANFIS controller is able to identify the nature of near-field or far-field of the earthquake and calculates the control force of each actuator at any moment. Simulation results show that the new adaptive controller is effective in reducing the critical responses of the structure such as peak/normed base shear, peak/normed mid-span displacement, and peak/normed acceleration. Furthermore, the parameters indicate that the index of damages to the structure has significantly decreased. The comparison of the bridge

response indices showed that the proposed method has yielded better results than the other previous methods. Since the proposed controller is designed with respect to a 3D model with the bending and nonlinear elements as well as the nonlinear control laws, its application to the bridge structure has no limitations, but needs to be investigated about other structures.

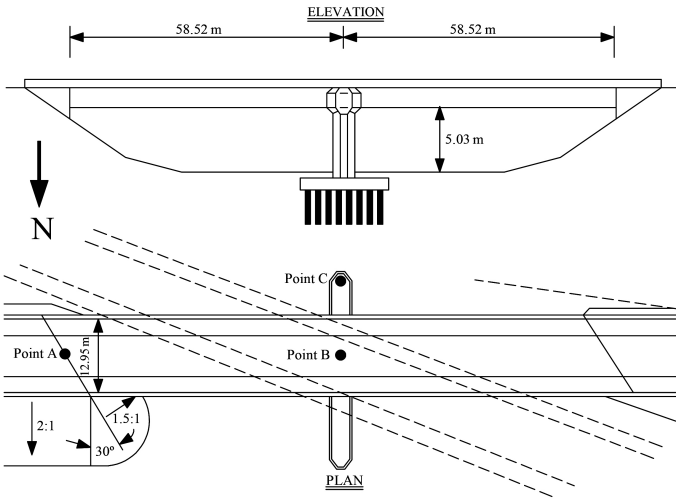


FIGURE 1. Elevation and plan views of 91/5 over-crossing [1].

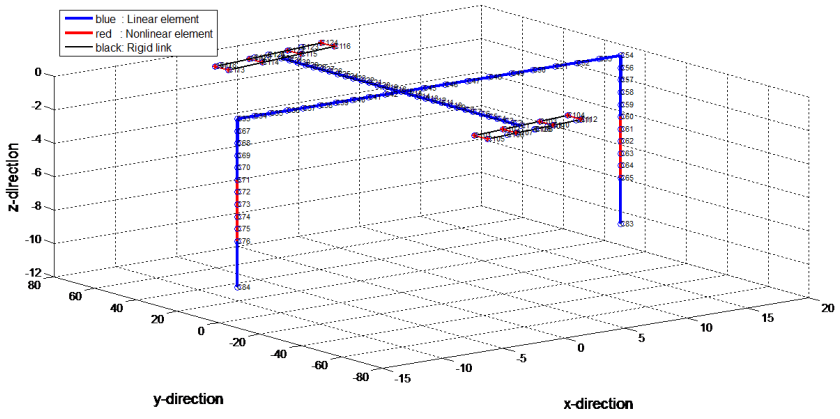


FIGURE 2. Finite element model of the bridge

FIGURE 3. Tug of war tournament

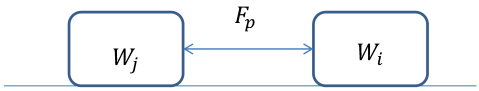


FIGURE 4. An idealized framework of tug of war [20]

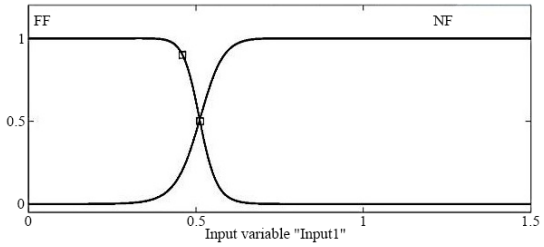


FIGURE 5. Membership functions of earthquake observer

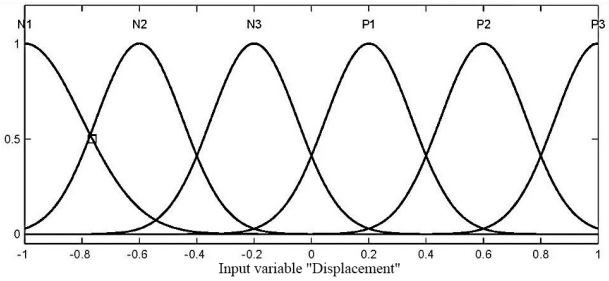


FIGURE 6. Input membership functions in ANFIS controller (Normalized displacement or Normalized acceleration)

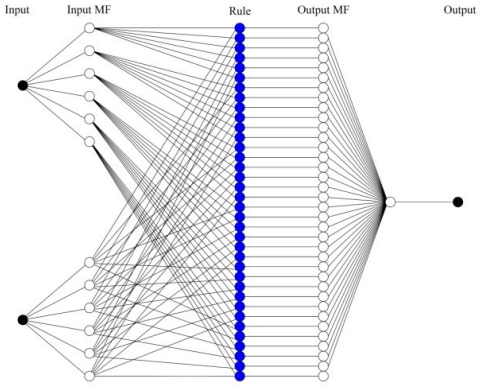


FIGURE 7. ANFIS configuration of the proposed controller

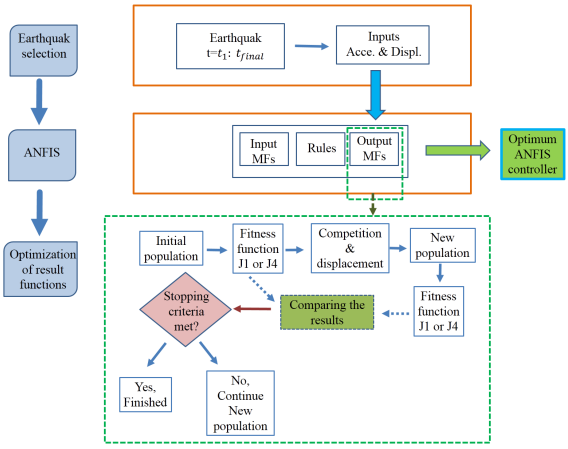


FIGURE 8. The applied methodology to design a nero-fuzzy optimized controller

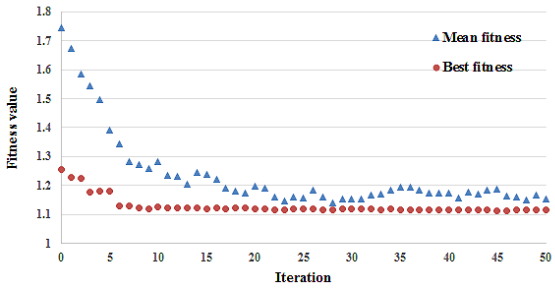


FIGURE 9. F-ANFIS controller optimization under N.P.Spr. earthquake with a factor of 1.5 and J1 index

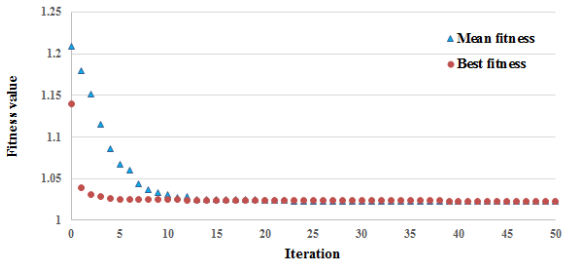


FIGURE 10. N-ANFIS controller optimization under Northridge earthquake with a factor of 1.5 and J1 index

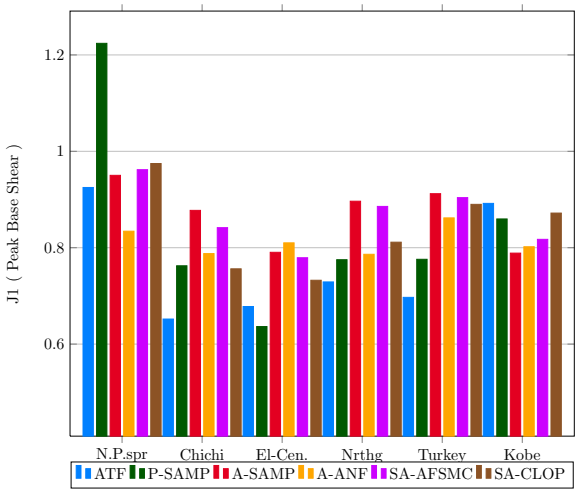


FIGURE 11. The J1 index comparison among the different control methods

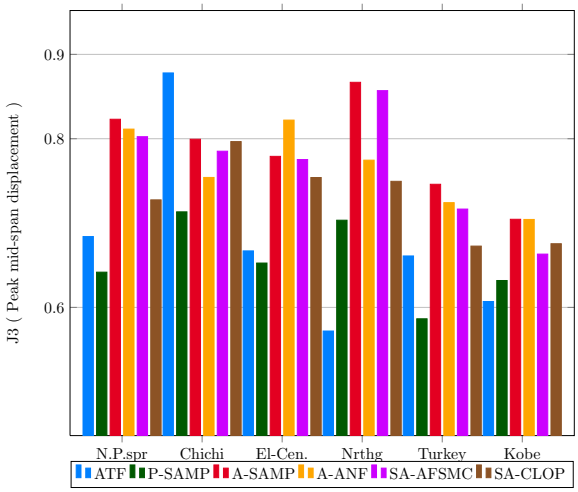


FIGURE 12. The J3 index comparison among the different control methods

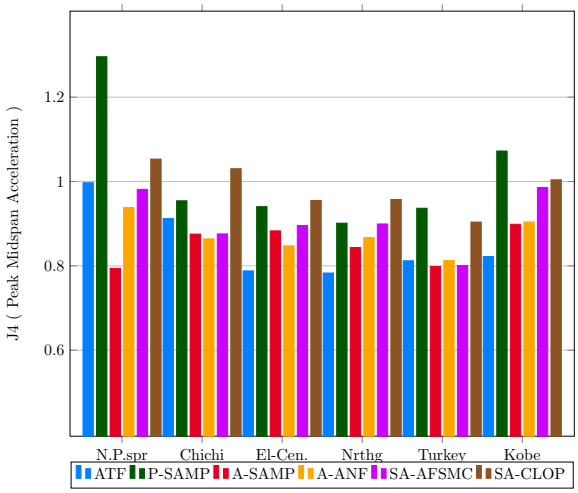


FIGURE 13. The J4 index comparison among the different control methods

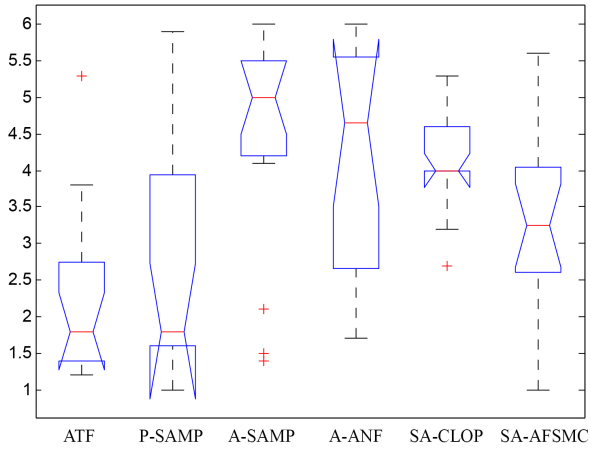


FIGURE 14. A view of the results of the Friedmans test

## REFERENCES

[1] A. K. Agrawal, P. Tan, S. Nagarajaiah and J. Zhang, Benchmark structural control problem for a seismically excited highway bridge-Part I: Phase I Problem definition, *Struct. Control Heal. Monit.*, **16** (2009), 509–529.

[2] S. Ali, *Semi-active Control of Earthquake Induced Vibrations in Structures Using Mr Dampers : Algorithm Development, Experimental Verification and Benchmark Applications*, Ph.D thesis, Indian Institute of Science, Bangalore, 560 012, 2008.

[3] J. M. Caicedo, S. J. Dyke, S. J. Moon, L. A. Bergman, G. Turan and S. Hague, Phase II benchmark control problem for seismic response of cable-stayed bridges, *Earthq. Eng. Eng. Vib.*, **16** (2017), 827–840.

[4] M. Dehghani, A. Seifi and H. Riahi-Madvar, Novel forecasting models for immediate-short-term to long-term influent flow prediction by combining ANFIS and grey wolf optimization, *J. Hydrol.*, **576** (2019), 698–725.

[5] S. J. Dyke, J. M. Caicedo, G. Turan, L. A. Bergman and S. Hague, Phase I benchmark control system for seismic response of cable-stayed bridges, *J. Struct. Eng.*, **129** (2003), 857–872.
[6] R. Eberhart and J. Kennedy, A new optimizer using particle swarm theory, *Proceedings of the Sixth International Symposium on Micro Machine and Human Science*, **12** (1995), 39-43.
[7] O. K. Erol and I. Eksin, A new optimization method: Big BangBig Crunch, *Adv. Eng. Softw.*, **37** (2006), 106–111.
[8] H. Ghaffarzadeh, Semi-active structural fuzzy control with MR dampers subjected to near-fault ground motions having forward directivity and fling step, *Smart Struct. Syst.*, **12** (2013), 595–617.
[9] A. Goli, H. Khademi Zareh, R. Tavakkoli-Moghaddam and A. Sadeghieh, A comprehensive model of demand prediction based on hybrid artificial intelligence and metaheuristic algorithms: A case study in dairy industry, *Int. J. Ind. Syst. Eng.*, **11** (2018), 190–203.
[10] M. S. Gonalves, R. H. Lopez and L. F. F. Miguel, Search group algorithm: A new metaheuristic method for the optimization of truss structures, *Comput. Struct.*, **153** (2015), 165-184.
[11] G. Heo, C. Kim, S. Jeon, C. Lee and J. Jeon, A hybrid seismic response control to improve performance of a two-span bridge, *Struct. Eng. Mech.*, **61** (2009), 675–684.
[12] R. S. Jangid and J. M. Kelly, Base isolation for near-fault motions, *Earthq. Eng. Struct. Dyn.*, **35** (2001), 691–707.
[13] S. Jaypuria, M. T. Ranjan and O. Jaypuria, Metaheuristic tuned ANFIS model for input-output modeling of friction stir welding, *Materials Today: Proceedings*, **18** (2019), 3922–3930.
[14] A. A. Kalteh and S. Babouei, Control chart patterns recognition using ANFIS with new training algorithm and intelligent utilization of shape and statistical features, *ISA Transactions*, **1** (2019).
[15] A. Kaveh and N. Khayatazad, A new meta-heuristic method: ray optimization, *Comput. Struct.*, **59** (2012), 283–294.
[16] A. Kaveh, S. M. Motie and M. Moslehi, Magnetic charged system search: a new meta-heuristic algorithm for optimization, *Acta Mech.*, **224** (2014), 85–107.
[17] A. Kaveh and N. Farhoudi, A new optimization method: dolphin echolocation, *Adv. Eng. Softw.*, **59** (2013), 53–70.
[18] A. Kaveh and A. Zolghadr, Democratic PSO for truss layout and size optimization with frequency constraints, *Comput. Struct.*, **130** (2014), 10–21.
[19] A. Kaveh and V. R. Mahdavi, Colliding bodies optimization: a novel meta-heuristic method, *Comput. Struct.*, **139** (2014), 18–27.
[20] A. Kaveh and A. Zolghadr, A novel meta-heuristic algorithm: TUG OF WAR optimization, *Iran Univ. Sci. Technol.*, **6** (2014), 469–492.
[21] S. Khalilpourazari and S. Khalilpourazari, Optimization of time, cost and surface roughness in grinding process using a robust multi-objective dragonfly algorithm, *Neural Comput. Appl.*, **1** (2018), 1–12.
[22] S. Khalilpourazari and H. R. Pasandideh, Modeling and optimization of multi-item multi-constrained EOQ model for growing items, *Knowl-Based Syst.*, **164** (2019), 150–162.
[23] S. Khalilpourazari, H. R. Pasandideh, H. R. Niaki and S. T. Akhavan Optimizing a multi-item economic order quantity problem with imperfect items, inspection errors, and backorders, *Soft Computing*, **23** (2019), 11671–11698.
[24] S. Khalilpourazari and H. R. Pasandideh, Sinecosine crow search algorithm: theory and applications, *Neural Comput. Appl.*, **1** (2019).
[25] S. Khalilpourazari, A. Mirzazadeh, G. W. Weber and H. R. Pasandideh, A robust fuzzy approach for constrained multi-product economic production quantity with imperfect items and rework process, *Optimization*, **69** (2020), 63–90.
[26] S. N. Madhekar and R. S. Jangid, Seismic performance of benchmark highway bridge installed with piezoelectric friction dampers, *IES J. Part A Civ. Struct. Eng.*, **4** (2011), 191–212.
[27] M. J. Mahmoodabadi, F. Farhadi and S. Sampour, Firefly algorithm based optimum design of vehicle suspension systems, *Int. J. Dyn. Control.*, **7** (2019), 134–146.
[28] G. P. Mavroeidis, G. Dong and A. S. Papageorgiou, Near-fault ground motions, and the response of elastic and inelastic single-degree-of-freedom(SDOF) systems, *Earthq. Eng. Struct. Dyn.*, **33** (2004), 1023–1049.
[29] S. Narasimhan, S. Nagarajaiah, H. Gavin and E. J. Johnson, Smart base-isolated benchmark building. Part I: Problem definition, *Struct. Control Heal. Monit.*, **13** (2006), 573-588.

[30] S. Narasimhan, S. Nagarajaiah and E. A.Johnson, Smart base-isolated benchmark building part IV: Phase II sample controllers for nonlinear isolation systems, *Struct. Control Heal. Monit.*, **15** (2008), 657–672.
[31] S. Narasimhan, Robust direct adaptive controller for the nonlinear highway bridge benchmark, *Struct. Control Heal. Monit.*, **16** (2009), 599–612.
[32] S. Nagarajaiah, S. Narasimhan, P. Tan and A. K. Agrawal, Benchmark structural control problem for a seismically excited highway bridge-Part III: Phase II Sample controller for the fully base-isolated case, *Struct. Control Heal. Monit.*, **16** (2009), 549–563.
[33] X. L. Ning, P. Tan, D. Y. Huang and F. L. Zhou, Application of adaptive fuzzy sliding mode control to a seismically excited highway bridge, *Struct. Control Heal. Monit.*, **16** (2009), 207–216.
[34] Y. Ohtori, R. E. Christenson, B. F. Spencer and S. J. Dyke, Benchmark control problems for seismically excited nonlinear buildings, *J. Eng. Mech.*, **130** (2004), 366–385.
[35] A. Preumont, M. Voltan, A. Sangiovanni, B. Mokrani and D. Alaluf, Active tendon control of suspension bridges, *Smart Struct. Syst.*, **18** (2016), 31–52.
[36] A. Sadollah, H. Eskandar, A. Bahreininejad and J. H. Kim, Water cycle, mine blast and improved mine blast algorithms for discrete sizing optimization of truss structures, *Comput. Struct.*, **149** (2015), 1–16.
[37] A. Saha, P. Saha and P. S. Kumar, Polynomial friction pendulum isolators (PFPIs) for seismic performance control of benchmark highway bridge, *Earthq. Eng. Eng. Vib.*, **16** (2017), 827–840.
[38] B. F. Spencer, S. J. Dyke and H. S. Deoskar, Benchmark problems in structural control: Part I Active Mass Driver system, *Earthq. Eng. Struct. Dyn.*, **27** (1998), 1127–1139.
[39] P. Tan and A. K. Agrawal, Benchmark structural control problem for a seismically excited highway bridge, Part II : Phase I Sample control designs, *Struct. Control Heal. Monit.*, **129** (2009), 857–872.
[40] J. N. Yang, A. K. Agrawal, B. Samali and J. C. Wu, Benchmark control problems for seismically excited nonlinear buildings, *J. Eng. Mech.*, **130** (2004), 437–446.

Received October 2019; $1^{st}$ revision January 2020; Final revision January 2020.

*E-mail address*: mostafa.ghelichi@gmail.com
*E-mail address*: ar.goltabar@nit.ac.ir
*E-mail address*: tavakoli@nit.ac.ir
*E-mail address*: akaramodin@yahoo.com